

Swarm-intelligent predictions of high-T_c polymorphs in monolayer CrI_3 above 77 K

Ying Luo(罗颖), Shuangyi Xu(许双旖), Yanan Wang(王亚南), and Yunwei Zhang(张云蔚)
Citation: Chin. Phys. B, 2025, 34 (**11**): 117105. DOI: 10.1088/1674-1056/addbcb
http://cpb.iphy.ac.cn; http://iopscience.iop.org/cpb

What follows is a list of articles you may be interested in

First-principles calculations on strain tunable hyperfine Stark shift of shallow donors in Si

Zi-Kai Zhou(周子凯) and Jun Kang(康俊)
Chin. Phys. B, 2025, 34 (**8**): 087102. DOI: 10.1088/1674-1056/addeba

Interacting Dirac semi-metal state in nonsymmorphic Kondo-lattice compound $CeAgSb_2$

Da-Liang Guo(郭达良), and Huan Li(黎欢)
Chin. Phys. B, 2025, 34 (**6**): 067102. DOI: 10.1088/1674-1056/adc6f6

Predicted stable two-dimensional semiconductor TiOS materials with promising photocatalytic properties: First-principles calculations

Pan Zhang(张攀), Shihai Fu(付世海), Chunying Pu(濮春英), Xin Tang(唐鑫), and Dawei Zhou(周大伟)
Chin. Phys. B, 2025, 34 (**5**): 057103. DOI: 10.1088/1674-1056/adb687

Structure prediction, electronic, and mechanical properties of alkali metal MB_{12} (*M= Be*, Mg, Ca, Sr) from first principles

Chun-Ying Pu(濮春英), Rong-Mei Yu(于荣梅), Ting Wang(王婷), Zhen-Yan X\"ue(薛振彦), Yong-Sheng Zhu(朱永胜), and Da-Wei Zhou(周大伟)
Chin. Phys. B, 2021, 30 (**1**): 017102. DOI: 10.1088/1674-1056/abb667

The role of CALYPSO in the discovery of high-T_c hydrogen-rich superconductors

Wenwen Cui(崔文文), Yinwei Li(李印威)
Chin. Phys. B, 2019, 28 (**10**): 107104. DOI: 10.1088/1674-1056/ab4253

Swarm-intelligent predictions of high-T_C polymorphs in monolayer CrI_3 above 77 K

Ying Luo(罗颖)[1,2], Shuangyi Xu(许双旖)[1,2], Yanan Wang(王亚南)[3,4,†], and Yunwei Zhang(张云蔚)[1,2,‡]

[1] *School of Physics, Sun Yat-sen University, Guangzhou* 510275, *China*
[2] *Guangdong Provincial Key Laboratory of Magnetoelectric Physics and Devices, Sun Yat-sen University, Guangzhou* 510275, *China*
[3] *Songshan Lake Materials Laboratory, Dongguan* 523808, *China*
[4] *Institute of Physics, Chinese Academy of Sciences, Beijing* 100190, *China*

(Received 25 March 2025; revised manuscript received 13 May 2025; accepted manuscript online 22 May 2025)

Monolayer CrI_3, crystalizing in the $P\bar{3}1m$ space group, is a prototypical two-dimensional (2D) material for observing intrinsic ferromagnetic order. However, its relatively low Curie temperature (T_C) of 45 K severely limits its practical applications, highlighting the need to explore novel metastable polymorphs with enhanced magnetic properties. In this study, we employ a global crystal structure search technique combined with first-principles calculations to systematically investigate new monolayer CrI_3 phases. Our structural predictions identify two novel polymorphs with Cm and $P2/m$ space groups, both of which are dynamically stable and exhibit significantly higher T_C values of 145 K and 81 K, respectively. Electronic property calculations show that the Cm phase is a half-metal, while the $P2/m$ phase is semiconducting with a bandgap of 0.14 eV. Monte Carlo simulations attribute these enhanced T_C values to a notable increase in exchange interactions. These findings expand the known phase space of CrI_3 and provide a promising pathway for designing high-temperature 2D ferromagnets for next-generation spintronic applications.

Keywords: chromium triiodide, 2D magnets, structure prediction, first-principles calculations, monolayer structure

PACS: 71.15.Mb, 71.20.–b, 63.20.dk, 75.50.Pp

DOI: 10.1088/1674-1056/addbcb **CSTR:** 32038.14.CPB.addbcb

1. Introduction

Two-dimensional (2D) materials with intrinsic magnetism have attracted significant attention in recent years due to their potential for providing robust or tunable magnetic properties.[1] Unlike layered materials, where magnetism is induced through external modifications, such as doping with magnetic atoms or proximity effects at interfaces,[2–4] the 2D materials with intrinsic magnetism offer a more stable platform for spintronic applications.[5] However, achieving long-range magnetic order in purely 2D systems is theoretically prohibited by the Mermin–Wagner theorem, which states that isotropic single atomic layers cannot sustain finite-temperature magnetism.[6]

This theoretical constraint was challenged in 2017 with the experimental discovery of intrinsic ferromagnetism in monolayer CrI_3 (Curie temperature $T_C = 45$ K)[7] and bilayer $Cr_2Ge_2Te_6$ ($T_C = 28$ K),[8] demonstrating that magnetic anisotropy can stabilize long-range order in low-dimensional systems. These breakthroughs not only validated the existence of intrinsic magnetic ordering in two dimensions, but also paved the way for the subsequent discovery of new 2D magnetic materials.[9–12]

The electronic and magnetic properties of 2D materials are highly sensitive to their structural polymorphs. For example, monolayer MoS_2 exists in both the metallic 1T and semiconducting 2H phases,[13] black phosphorene exhibits strong in-plane thermal anisotropy, whereas blue phosphorene is isotropic,[14] and $ReSe_2$ display layer-dependent optical anisotropy due to their distorted octahedral coordination.[15] Modern phase engineering,[16] powered by computational structure prediction tools, has accelerated the discovery of metastable polymorphs in various 2D systems, such as graphene,[17] boron nitrides,[18] and transition metal chalcogenides.[19] These advances suggest that unexplored structural configurations of known 2D magnets could host enhanced magnetic coupling, leading to higher magnetic transition temperatures.

Chromium triiodide (CrI_3), a prototypical van der Waals ferromagnet, exemplifies this potential. Monolayer CrI_3 (space group $P\bar{3}1m$) exhibits intrinsic Ising ferromagnetism with a T_C of 45 K[7] and a bandgap of 1.2 eV,[20–23] enabling its integration into heterostructures with topological insulators, valley-polarized systems, and superconductors.[24–30] However, its relatively low T_C (below the liquid nitrogen temperature) severely restricts its practical applications. While approaches such as strain engineering and heterostructuring have

†Corresponding author. E-mail: wangyanan@sslab.org.cn
‡Corresponding author. E-mail: zhangyunw@mail.sysu.edu.cn

© 2025 Chinese Physical Society and IOP Publishing Ltd. All rights, including for text and data mining, AI training, and similar technologies, are reserved.

been theoretically explored to enhance its T_C to 91 K,[31] the intrinsic potential of metastable CrI_3 polymorphs with optimized exchange interactions and magnetic anisotropy remains unexplored.

Here, we employ a swarm-intelligent global structure search method (CALYPSO)[32–35] combined with first-principles calculations to systematically explore novel monolayer CrI_3 polymorphs. Our search identifies two new metastable phases, *Cm* and $P2/m$, that exhibit significantly higher T_C of 145 K and 81 K, respectively, surpassing the experimentally observed 45 K in the $P\bar{3}1m$ phase. Electronic structure calculations reveal that the *Cm*-phase is a half-metal with strong spin polarization, while the $P2/m$-phase retains semiconducting with a bandgap of 0.14 eV. Both phases exhibit enhanced magnetic anisotropic energy (MAE) and stronger exchange interactions, which account for their higher T_C values. Our work not only expands the known phase space of CrI_3 but also established a promising way for designing high-performance 2D magnet through metastable polymorph discovery.

2. Computational methods

The swarm-intelligence-based CALYPSO method and code were employed for searching low-energy 2D monolayers.[36–39] Its validity has been manifested by successful identification of the ground-state structures for a large number of systems. In our CALYPSO calculations, simulation cells containing up to two formula units were considered. The population size was set to 30, and more than 900 structures were sampled on the potential energy surface for each stoichiometry within the 2D planar space.

Energy calculations and structural optimizations were conducted using density functional theory (DFT) as implemented in the Vienna *Ab Initio* Simulation Package (VASP).[40] The ion–electron interactions were described using the projector-augmented plane wave (PAW) method,[41] and the electron exchange–correlation effects were treated with the generalized gradient approximation (GGA) formulated by Perdew, Burke, and Ernzerhof (PBE).[42] A plane-wave energy cutoff of 520 eV and a Monkhorst–Pack Brillouin zone sampling grid with a resolution of $2\pi \times 0.03$ Å^{-1} were adopted to ensure that all enthalpy calculations are well converged with an error less than 1 meV/atom. Structural relaxations were performed with forces converged to less than 0.001 eV·Å^{-1}.

The monolayers were oriented in the *xy*-plane, with the *z*-axis perpendicular to the layer. A vacuum spacing of 20 Å was introduced along the *z* direction to eliminate interactions between layers. To account for electron correlation effects in the Cr-3d orbitals, the DFT+U method was employed.[43,44] The Hubbard U value of 2.7 eV and exchange parameter J of 0.7 eV were carefully chosen to reproduce key experimentally observations of the CrI_3 system, including the correct orientation of the easy magnetization axis. These parameters have also been used and validated in previous theoretical studies on CrI_3.[45,46] Phonon calculations were performed using the frozen phonon method, as implemented in the PHONOPY package.[47]

3. Results and discussion

Our structural search identifies two novel monolayer polymorphs, *Cm* and $P2/m$, each exhibiting distinct structural characteristics. The *Cm* phase features a trigonal bipyramidal coordination, wherein each Cr atom is bonded to five iodine atoms, forming a five-faced triangular pyramid (Fig. 1(a)). The $P2/m$ phase adopts an octahedral configuration, with each Cr atom surrounded by six iodine atoms, resulting in a more symmetrical structural arrangement (Fig. 1(b)).

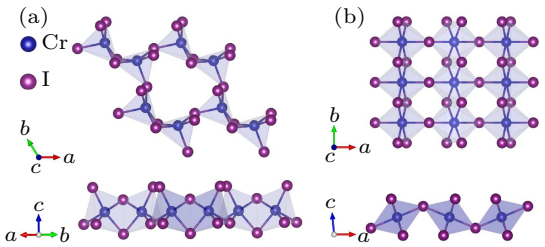


Fig. 1. Predicted monolayer CrI_3 structures with the space groups *Cm* (a) and $P2/m$ (b).

Table 1. Structural information of the *Cm* and $P2/m$ phases of monolayer CrI_3.

Space group	Lattice parameters (Å)	Atomic coordinates (fractional)
Cm	$a = 7.351$	Cr 0.058 0.340 0.507
	$b = 5.533$	0.340 0.058 0.507
	$c = 21.570$	I 0.358 0.910 0.400
	$\alpha = \beta = 90.884$	0.910 0.358 0.400
	$\gamma = 116.360$	0.112 0.693 0.561
		0.692 0.112 0.561
		0.421 0.421 0.458
		0.210 0.210 0.605
$P2/m$	$a = 10.371$	Cr 0.000 0.000 0.500
	$b = 3.983$	0.500 0.000 0.500
	$c = 19.920$	I 0.459 0.500 0.590
	$\alpha = 90.000$	0.541 0.500 0.410
	$\beta = 94.980$	0.071 0.500 0.590
	$\gamma = 90.000$	0.929 0.500 0.410
		0.759 0.000 0.554
		0.241 0.000 0.446

The energy differences (ΔE) of the *Cm* and $P2/m$ phases relative to the ground-state $P\bar{3}1m$ phase are 0.178 eV/atom and 0.079 eV/atom, respectively, indicating their relative energetic favorability. Notably, these ΔE values are lower than those of several experimentally synthesized metastable 2D materials, for example, the 1T phase of MoS_2 ($\Delta E = 0.280$ eV/atom) and the *Imm*2 phase of GaAs ($\Delta E = 0.348$ eV/atom).[48–51] To further evaluate their thermodynamic stability, we calculated the formation energies of the *Cm* and $P2/m$ phases with respect to elemental Cr and I. The calculated formation energies

are −0.569 eV/atom for the *Cm* phase and −0.668 eV/atom for the $P2/m$ phase. These negative values indicate that both phases are thermodynamically stable against decomposition into their elemental constituents. Therefore, despite being metastable with respect to the ground state, the moderate formation energies suggest that the *Cm* and $P2/m$ phases could potentially be synthesized using appropriate techniques, such as molecular beam epitaxy. Additionally, phonon dispersion calculations are performed to assess their dynamic stability (Figs. 2(a) and 2(b)). The absence of imaginary frequencies along the high-symmetry paths in the Brillouin zone confirms that both the *Cm* and $P2/m$ phases are dynamically stable.

Next, we investigated the electronic and magnetic properties of the two newly identified CrI_3 monolayers. To determine their magnetic ground state, we performed total energy calculations for four common magnetic configurations in both the *Cm* and $P2/m$ phases: ferromagnetic (FM) and three antiferromagnetic states (AFM1, AFM2, and AFM3) (Figs. 3(a) and 3(b)). The results indicate that both phases favor ferromagnetic ordering in their magnetic ground states. The calculated energies for these four magnetic configurations are listed in Table 2. Additionally, both phases exhibit identical magnetic moments to the experimental $P\bar{3}1m$ phase of around 6.0 μ_B per unit cell, suggesting the robustness of their ferromagnetic behavior.

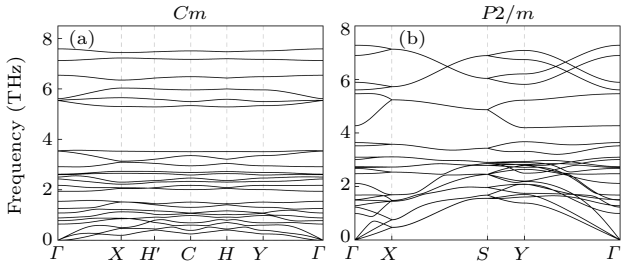


Fig. 2. Calculated phonon dispersion spectra of the *Cm* phase (a) and $P2/m$ phase (b). The absence of imaginary frequencies along the high-symmetry paths in the Brillouin zone confirms their dynamic stability.

Table 2. The relative energies (in units of meV/atom) between FM and the three configurations (AFM1, AFM2, and AFM3).

Space group	FM (meV)	AFM1 (meV)	AFM2 (meV)	AFM3 (meV)
Cm	0	19.38	7.05	13.55
$P2/m$	0	5.19	5.54	8.93

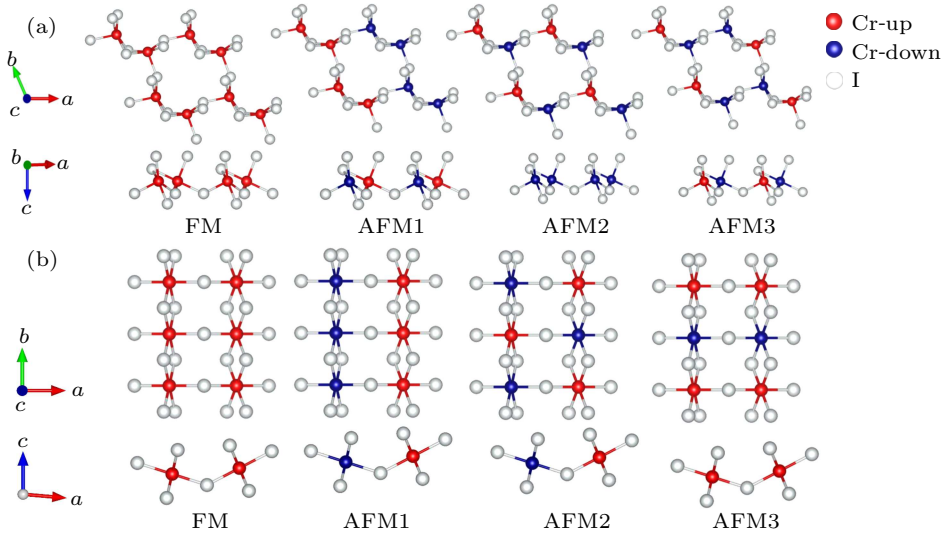


Fig. 3. Four magnetic configuration considered for the *Cm* phase (a) and $P2/m$ phase (b) of CrI_3.

Table 3. Magnetic anisotropy energy (MAE), exchange interactions (J_1, J_2, J_3), and Curie temperature (T_C) for *Cm*, *P2/m*, and experimental $P\bar{3}1m$ phases in the monolayer CrI_3 system.

Space group	MAE (meV)	J_1 (meV)	J_2 (meV)	J_3 (meV)	A_D (meV)	T_C (K)
Cm	–1.20	11.67	13.47	1.14	–0.53	145
$P2/m$	0.72	4.63	4.29	0.45	0.32	81
$P\bar{3}1m$	0.65[46]	2.93	0.64	–0.16	0.14	45 (Exp.)

Band structures and densities of states calculations reveal that both phases exhibit spin polarization. The *Cm* phase demonstrates half-metallic behavior, featuring a significant energy gap of 2.19 eV at the Fermi level in the spin-down states. While the $P2/m$ phase displays semiconducting properties with a band gap of 0.14 eV. Further analysis of the densities of states indicates that the magnetic properties in ferromagnetic state are primarily driven by the hybridization between Cr-3d orbitals and I-5p orbitals.

Magnetic anisotropy energy (MAE) is a critical parameter for stabilizing 2D magnetism at finite temperatures, as it quantifies the energy difference between in-plane and out-of-plane spin orientations by incorporating spin–orbit coupling (SOC) ($E_{MAE} = E^{SOC}_{100} - E^{SOC}_{001}$). Our calculations show that both the

Cm and $P2/m$ phases have stronger magnetic anisotropy than the experimental $P\bar{3}1m$ phase (Table 3). The MAE values for the *Cm* and $P2/m$ phases are -1.20 meV and 0.72 meV per Cr atom, respectively. These are 0.59 meV and 0.11 meV higher than the value for the experimental $P\bar{3}1m$ phase.[46] For the *Cm* phase, the negative MAE value indicates that the easy magnetization axis lies in the in-plane (100) direction, while for the $P2/m$ phase, the positive MAE value suggests that the easy magnetization axis is aligned with the out-of-plane (001) direction.

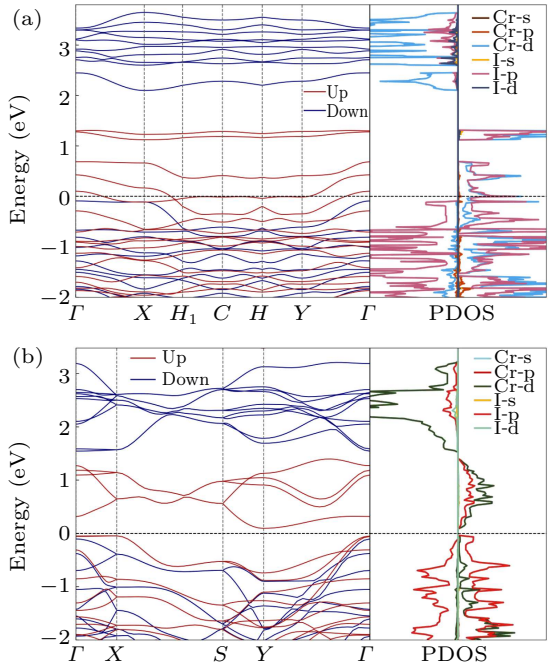


Fig. 4. Band structures and projected density of states (PDOS) for the *Cm* phase (a) and $P2/m$ phase (b). The black dashed lines indicate the Fermi level in each panel.

We further performed an orbital-resolved analysis to gain a deeper understanding of the fundamental mechanisms underlying the MAE. As shown in Figs. 5(a) and 5(c), the contributions from orbital hybridizations involving Cr atoms are minimal due to the d's sub-orbitals mutually cancel each other out in both phases. In the *Cm* phase, the positive MAE is primarily due to the hybridization between the p_y and p_z orbitals of iodine atoms, while negative contributions arise from the hybridizations between the p_x and p_y orbitals, as well as the p_x andp_z orbitals of iodine atoms (Fig. 5(b)). In the $P2/m$ phase, the positive MAE is mainly attributed to the hybridization between the p_x and p_y orbitals of iodine atoms (Fig. 5(d)). These results demonstrate the critical role of iodine orbital hybridization in governing the magnetic anisotropy of the two phases.

We evaluate T_C using Metropolis Monte Carlo simulations based on the Heisenberg model. Considering the nearest, second, and third neighbor couplings of on-site spins, the spin Hamiltonian can be written as

$$H = -\sum_{\langle i,j\rangle} J_1 S_i \cdot S_j - \sum_{\langle\langle i,j\rangle\rangle} J_2 S_i \cdot S_j - \sum_{\langle\langle\langle i,j\rangle\rangle\rangle} J_3 S_i \cdot S_j - \sum_i A_D (S_i^z)^2, \quad (1)$$

where $\langle i,j\rangle$, $\langle\langle i,j\rangle\rangle$ and $\langle\langle\langle i,j\rangle\rangle\rangle$ denote the nearest, second, and third neighbor spins, respectively. J_1, J_2, and J_3 are the corresponding Heisenberg exchange interaction constants. A_D represents the single-ion anisotropy. The total energies of the different magnetic configurations are calculated using DFT to obtain the values of J_1, J_2, and J_3. The value of A_D is derived from the magnetic anisotropy energy.

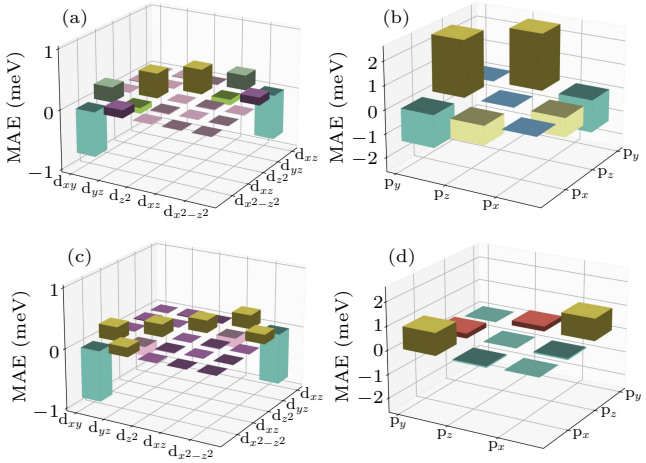


Fig. 5. Orbital-resolved SOC-MAE contributions: Panels (a) and (b) are the Cr-3d and I-5p orbitals of the *Cm* phase. Panels (c) and (d) are the Cr-3d and I-5p orbitals of the $P2/m$ (c) phase.

We performed Monte Carlo simulations on an $80 \times 80 \times 1$ spin lattice for the *Cm* phase and a $40 \times 40 \times 1$ spin lattice for the $P2/m$ phase with periodic boundary conditions, using 10^5 steps for equilibration and averaging. In our Monte Carlo simulations, the T_C is determined from the peaks in the specific heat capacity as a function of temperature. To validate our Monte Carlo simulations, we benchmarked the method by calculating the T_C of two experimentally synthesized materials: the $P\bar{3}1m$ phase of CrI_3 (experimental $T_C = 45$ K)[7] and the $R\bar{3}m$ phase of Gd_2C (experimental $T_C = 350$ K).[52] Our simulations yielded T_C values of 58 K for CrI_3 and 370 K for Gd_2C, demonstrating good agreement with experimental results. In particular, our predicted T_C for the $P\bar{3}1m$ phase of CrI_3 is also consistent with previously reported Monte Carlo simulation results[53–55]

As shown in Table 3, the calculated values of J_1, J_2, and J_3 are all positive, indicating that the magnetic couplings favor ferromagnetic ordering.

Figure 6 illustrates the evolution of the Monte Carlo spin moments and the corresponding heat capacity curves for *Cm* and $P2/m$ phases. The simulated T_C values for the *Cm* and

$P2/m$ phases are 145 K and 81 K, respectively, significantly higher than that of 45 K observed in the experimental structure. These results suggest that both Cm and $P2/m$ phases are promising candidates for further exploration within the monolayer CrI_3 system and hold considerable potential for advancing research on 2D magnetic materials.

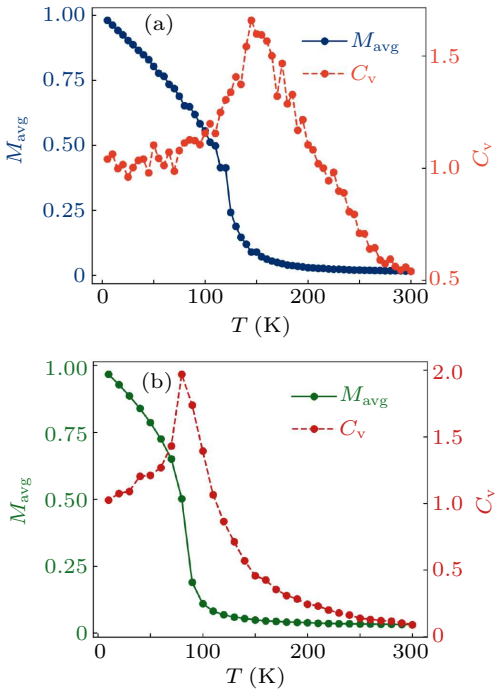


Fig. 6. Temperature dependence of the average magnetic moment (M_{avg}) and specific heat (C_v) for the Cm phase (a) and $P2/m$ phase (b), as obtained from Monte Carlo simulations. The Curie temperatures (T_C) of the Cm and $P2/m$ phases are 145 K and 81 K, respectively.

4. Conclusions

In conclusion, we systematically explore novel phases within the monolayer CrI_3 system by combining a swarm intelligence global structure search methodology with first-principles calculations. This approach leads to the identification of two previously unreported phases, Cm and $P2/m$, which exhibit significantly enhanced T_C values of 145 K and 81 K, respectively, well beyond the experimentally observed value of 45 K. Additionally, we show that the Cm phase is half-metallic, while the $P2/m$ phase exhibit semiconducting properties. The insights gained from this work not only deepen our understanding of the various electronic and magnetic properties in the monolayer CrI_3 system, but also provide a promising foundation for the development of high-performance spintronic materials.

Acknowledgements

Project supported by the National Key Research and Development Program of China (Grant No. 2023YFA1610000), the National Natural Science Foundation of China (Grant Nos. 12304036 and 12304265), the Basic and Applied Basic Research Foundation of Guangdong Province, China (Grant No. 2023A1515010071), and the Fundamental Research Funds for the Central Universities to Sun Yat-sen University (Grant No. 23xkjc016).

References

[1] Ma Q, Ren G, Xu K and Ou J Z 2021 *Adv. Opt. Mater.* **9** 2001313
[2] González-Herrero H, Gómez-Rodríguez J M, Mallet P, Moaied M, Palacios J J, Salgado C, Ugeda M M, Veuillen J Y and Brihuega I 2016 *Science* **352** 437
[3] Son Y W, Cohen M L and Louie S G 2006 *Nature* **444** 347
[4] Liu H, Sun J T, Fu H X, Sun P J, Feng Y P and Meng S 2017 *ChemPhysChem* **18** 1916
[5] Ahn E C 2020 *npj 2D Mater. Appl.* **4** 17
[6] Mermin N D and Wagner H 1966 *Phys. Rev. Lett.* **17** 1133
[7] Huang B, Clark G, Navarro-Moratalla E, Klein D R, Cheng R, Seyler K L, Zhong D, Schmidgall E, McGuire M A and Cobden D H 2017 *Nature* **546** 270
[8] Gong C, Li L, Li Z, Ji H, Stern A, Xia Y, Cao T, Bao W, Wang C, Wang Y, Qiu Z Q, Cava R J, Louie S G, Xia J and Zhang X 2017 *Nature* **546** 265
[9] Ju H, Lee Y, Kim K T, Choi I H, Roh C J, Son S, Park P, Kim J H, Jung T S, Kim J H, Kim K H, Park J G and Lee J S 2021 *Nano Lett.* **21** 5126
[10] Song Q, Occhialini C A, Ergeçen E, Ilyas B, Amoroso D, Barone P, Kapeghian J, Watanabe K, Taniguchi T, Botana A S, Picozzi S, Gedik N and Comin R 2022 *Nature* **602** 601
[11] Lee K, Dismukes A H, Telford E J, Wiscons R A, Wang J, Xu X, Nuckolls C, Dean C R, Roy X and Zhu X 2021 *Nano Lett.* **21** 3511
[12] Cheng M, Hu Q, Huang Y, Ding C, Qiang X B, Hua C, Fang H, Lu J, Peng Y, Yang J, Xi C, Pi L, Watanabe K, Taniguchi T, Lu H Z, Novoselov K S, Lu Y and Zheng Y 2024 *Nat. Phys.* **20** 1973
[13] Lin Y C, Dumcenco D O, Huang Y S and Suenaga K 2014 *Nat. Nanotechnol.* **9** 391
[14] Jain A and McGaughey A J H 2015 *Sci. Rep.* **5** 8501
[15] Zhao H, Wu J, Zhong H, Guo Q, Wang X, Xia F, Yang L, Tan P and Wang H 2015 *Nano Res.* **8** 3651
[16] Kim D, Pandey J, Jeong J, Cho W, Lee S, Cho S and Yang H 2023 *Chem. Rev.* **123** 11230
[17] Kumar R, Joanni E, Singh R K, Singh D P and Moshkalev S A 2018 *Prog. Energy Combust. Sci.* **67** 115
[18] Jiang X F, Weng Q, Wang X B, Li X, Zhang J, Golberg D and Bando Y 2015 *J. Mater. Sci. Technol.* **31** 589
[19] Chhowalla M, Liu Z and Zhang H 2015 *Chem. Soc. Rev.* **44** 2584
[20] Wu Z W, Yu J and Yuan S J 2019 *Phys. Chem. Chem. Phys.* **21** 7750
[21] Zhang W B, Qu Q, Zhu P and Lam C H 2015 *J. Mater. Chem. C* **3** 12457
[22] Dillon Jr J F and Olson C E 1965 *J. Appl. Phys.* **36** 1259
[23] Li P, Wang C, Zhang J, Chen S, Guo D, Ji W and Zhong D 2020 *Sci. Bull.* **65** 1064
[24] Hou Y, Kim J and Wu R 2019 *Sci. Adv.* **5** eaaw1874
[25] Zhai B X, Du J, Shen C H, Wang T X, Peng Y T, Zhang Q M and Xia C X 2019 *Phys. Rev. B* **100** 195307
[26] Hidalgo-Sacoto R, Gonzalez R I, Vogel E E, Allende S, Mella J D, Cardenas C, Troncoso R E and Munoz F 2020 *Phys. Rev. B* **101** 205425
[27] Hu T, Zhao G D, Gao H, Wu Y B, Hong J S, Stroppa A and Ren W 2020 *Phys. Rev. B* **101** 125401
[28] Lu Y, Fei R X, Lu X B, Zhu L H, Wang L and Yang L 2020 *ACS Appl. Mater. Interfaces* **12** 6243
[29] Margalit G, Yan B and Oreg Y 2020 *Phys. Rev. B* **102** 024515
[30] Su T, Lohmann M, Li J X, Xu Y D, Niu B, Alghamdi M, Zhou H D, Cui Y T, Cheng R and Taniguchi T 2020 *2D Mater.* **7** 045006
[31] Wu Z, Shen Z, Xue Y and Song C 2022 *Phys. Rev. Mater.* **6** 014011
[32] Luo X Y, Yang J H, Liu H Y, Wu X J, Wang Y C, Ma Y M, Wei S H, Gong X G and Xiang H J 2011 *J. Am. Chem. Soc.* **133** 16285
[33] Wang Y C, Lv J, Zhu L and Ma Y M 2010 *Phys. Rev. B* **82** 094116
[34] Wang Y C, Miao M S, Lv J, Zhu L, Yin K T, Liu H Y and Ma Y M 2012 *J. Chem. Phys.* **137** 224110

[35] Wang Y C, Lv J, Zhu L and Ma Y M 2012 *Comput. Phys. Commun.* **183** 2063
[36] Miao N and Sun Z 2022 *WIREs Comput. Mol. Sci.* **12** e1545
[37] Gao P, Gao B, Lu S, Liu H, Lv J, Wang Y and Ma Y 2022 *Front. Phys.* **17** 23203
[38] Tang C, Kour G and Du A 2019 *Chin. Phys. B* **28** 107306
[39] Huang C, Feng J, Wu F, Ahmed D, Huang B, Xiang H, Deng K and Kan E 2018 *J. Am. Chem. Soc.* **140** 11519
[40] Kresse G and Furthmúller J 1996 *Phys. Rev. B* **54** 11169
[41] Kresse G and Joubert D 1999 *Phys. Rev. B* **59** 1758
[42] Perdew J P, Burke K and Ernzerhof M 1996 *Phys. Rev. Lett.* **77** 3865
[43] Anisimov V I, Zaanen J and Andersen O K 1991 *Phys. Rev. B* **44** 943
[44] Dudarev S L, Botton G A, Savrasov S Y, Humphreys C J and Sutton A P 1998 *Phys. Rev. B* **57** 1505
[45] Wu Z W, Yu J and Yuan S J 2019 *Phys. Chem. Chem. Phys.* **21** 7750
[46] Lado J L and Fernández-Rossier J 2017 2*D Mater.* **4** 035002
[47] Togo A and Tanaka I 2015 *Scr. Mater.* **108** 1
[48] Persson K A https://www.osti.gov/servlets/purl/1270385 [2025-05-12]
[49] Persson K A https://www.osti.gov/servlets/purl/1190621 [2025-05-12]
[50] Persson K A https://www.osti.gov/servlets/purl/1277364 [2025-05-12]
[51] Persson K A https://www.osti.gov/servlets/purl/1200591 [2025-05-12]
[52] Lee S Y, Hwang J Y, Park J, Nandadasa C N, Kim Y, Bang J, *et al.* 2020 *Nat. Commun.* **11** 1526
[53] Xue F, Hou Y S, Wang Z and Wu R Q 2019 *Phys. Rev. B* **100** 224429
[54] Huang C X, Feng J S, Wu F, Ahmed D, Huang B, Xiang H J, Deng K M and Kan E J 2018 *J. Am. Chem. Soc.* **140** 11519
[55] Zhang W B, Qu Q, Zhu P and Lam C H 2015 *J. Mater. Chem. C* **3** 12457